

# Noise analysis and sensitivity enhancement in immunomagnetic nanomechanical biosensors

Kutay Icoz,<sup>1,2</sup> Brian D. Iverson,<sup>2,3</sup> and Cagri Savran<sup>1,2,3,4,a)</sup>

<sup>1</sup>Weldon School of Biomedical Engineering, Purdue University, Indiana 47907, USA

<sup>2</sup>Birck Nanotechnology Center, Purdue University, Indiana 47907, USA

<sup>3</sup>School of Mechanical Engineering, Purdue University, Indiana 47907, USA

<sup>4</sup>School of Electrical and Computer Engineering, Purdue University, Indiana 47907, USA

(Received 12 May 2008; accepted 20 August 2008; published online 11 September 2008)

We report noise and detection limitations in cantilever-based immunomagnetic biosensors. A differential cantilever system with sensing and control arms was used whereby the control arm was passivated with bovine serum albumin (BSA) and the sensing arm was functionalized with biotin-BSA. Streptavidin-coated magnetic beads were exposed to cantilever arms. An oscillatory magnetic field induced a magnetic force on the beads which caused a relative deflection of the sensing arm. Increasing the excitation frequency suppressed the  $1/f$  noise by 100-fold, resulting in a deflection resolution of  $0.065 \text{ \AA}$  in air. © 2008 American Institute of Physics.

[DOI: 10.1063/1.2980036]

Detection of biomolecules and cells is crucial for biological and medical research and for early diagnosis of diseases. Among the various methods available, cantilever systems have attracted significant attention due to their label-free nature and miniaturization potential. Numerous cantilever-based biosensor applications have already been demonstrated.<sup>1-7</sup> Optical, electrical, and magnetic systems have been employed for measuring the static deflection of cantilevers or resonant frequency shifts as a result of biological binding.<sup>3,4,6,8,9</sup>

Researchers have been pursuing various methods to enhance detection sensitivity in cantilever-based sensors such as external actuation<sup>6</sup> or significantly reducing cantilever dimensions.<sup>10</sup> However, reduction in surface area also reduces the ability for particles in solution to selectively swim and bind to these smaller devices (this is especially true for low concentrations).

Magnetic excitation of atomic force microscopy cantilevers was studied by Lindsay *et al.*<sup>11</sup> Later on, Baselt *et al.*<sup>12</sup> proposed magnetic-bead-assisted biosensing whose application to DNA and telomerase detection was demonstrated by Weizmann *et al.*<sup>13</sup> Immunomagnetic cantilever sensors offer significant advantages: (1) cantilever-based systems can be readily combined with immunomagnetic separation to isolate biomolecules from complex biological mixtures, circumventing the need to directly expose the mixtures to the cantilevers; (2) a small number of entities that would otherwise not cause a significant mass change (required for resonant frequency shift measurement techniques) may be detected by forcing the cantilever to bend above background noise levels. In this letter, we analyze noise and certain detection limitations in immunomagnetic cantilever sensors, demonstrate improvement in minimum detectable deflection (MDD), and discuss the effects of physical parameters of the system on the minimum number of detectable beads.

The noise spectrum for an interdigitated cantilever-based system similar to the one studied here has been explained previously.<sup>14,15</sup> At low frequencies, flicker, i.e.,  $1/f$  type noise is dominant and results in poor resolution for slow,

dc-type excitations. To overcome these limitations we employed magnetic beads in conjunction with oscillating magnetic fields to actuate the cantilever in air at high frequencies where flicker noise is minimal. This approach allows standard microfabricated cantilevers (with typical dimensions of hundreds of microns) to detect extremely small deflections that result from binding of target-loaded magnetic beads.

A schematic of the detection system is shown in Fig. 1. Magnetic beads, that can be functionalized to specifically bind to biological agents, are captured on the surface of the sensing arm of two neighboring cantilevers. An alternating magnetic field from an electromagnet exerts a force on the beads resulting in oscillatory bending of the sensing arm. Interferometry is used to measure the relative deflection between the interdigitated fingers attached to the neighboring cantilevers. A laser beam reflected from the interdigitated fingers produces diffraction modes whose intensities depend on the relative distance between the cantilevers. Two photodetectors are used to detect the intensities of the zeroth and first order diffraction modes which have a periodic dependence on the relative vertical displacement of moving (sensing) fingers with respect to reference fingers.<sup>14-16</sup>

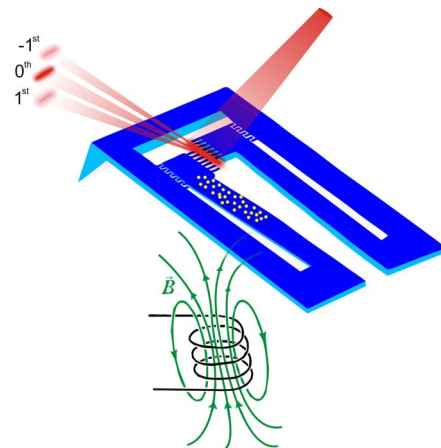


FIG. 1. (Color online) Schematic of the detection system. The presence of magnetic beads on the sensing arm causes a differential deflection relative to the reference arm upon applying a magnetic field. The differential motion is detected directly using interferometry.

<sup>a)</sup>Electronic mail: savran@purdue.edu.

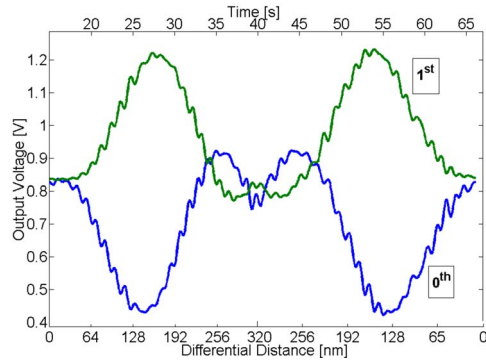


FIG. 2. (Color online) Calibration curves showing the intensities of zeroth and first diffraction modes. The input voltage is increased at discrete times (indicated by transient overshoots) from 0 to 20 V ( $\sim 0$ –320 nm) and decreased back to 0 V. To measure small deflections, the system is biased at the maximum sensitivity point ( $\sim 208$  nm relative deflection).

Figure 2 illustrates the calibration curves of the photodetector voltages as a function of time and relative deflection for zeroth and first order diffraction modes. For this study, a silicon-rich silicon nitride cantilever pair was used (density  $\rho=2900$  kg/m<sup>3</sup>, Young's modulus  $E=200$  GPa, length  $L=500$   $\mu$ m, width  $w=100$   $\mu$ m, thickness  $t=1$   $\mu$ m, and quality factor  $Q=20$ ). Calibration curves were obtained by increasing the magnitude of the magnetic field at 1 s time intervals and observing the photodetector voltages. The field strength was increased by increasing the voltage input to the electromagnet until the relative cantilever deflection was 320 nm in order to fully observe the maxima and minima. Decreasing the fields resulted in a symmetric response. For maximum sensitivity, the differential cantilevers were biased near the point where the slope is a maximum ( $\sim 208$  nm). The first mode was used as a confirmation of the zeroth mode's behavior and as a check for the alignment accuracy. After obtaining the calibration curves and the biasing, only the zeroth mode's signal was considered.

We performed experiments to investigate the noise in the system while simultaneously demonstrating its potential for biological detection. The reference cantilever was coated with bovine serum albumin (BSA) [Sigma-Aldrich, 3 mg/ml in phosphate buffered saline (PBS) (GIBCO)] and the sensing cantilever was coated with biotin-coupled BSA (B-BSA) (Pierce, 2 mg/ml, in PBS) using a nanojet dispenser (Micro-Fab Tech). Droplets of approximately 1 nl were continuously dispensed to keep the cantilever arms wet for 15 min. Both reference and sensing arms were exposed to droplets of streptavidin-coated magnetic bead suspensions. Cantilever arms were washed with PBS and de-ionized water leaving the B-BSA arm with magnetic beads bound to the surface [see Fig. 3(a)]. Cantilevers were then dried for imaging and measurements. About 30% more beads bound to the B-BSA (sensing) cantilever than the BSA-coated cantilever ( $\sim 13$  000 versus  $\sim 10$  000, image processing for bead count performed in MATLAB). Many beads bound nonspecifically to the BSA-coated cantilever, indicating the imperfect passivation of the reference arm. Although not the main focus of this study, this is an excellent demonstration of the advantage of utilizing an inherently differential detection system which automatically suppresses the effect of nonspecific binding thereby revealing a signal that is only due to the difference between the two cantilevers. Hence, this cantilever pair was intentionally used for the noise analysis as opposed to an

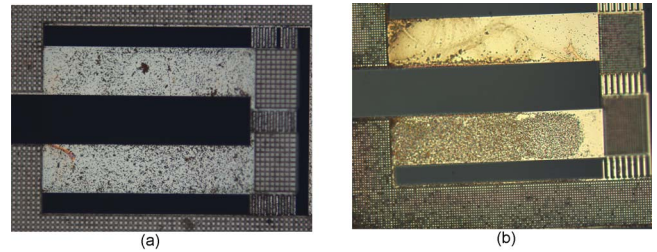


FIG. 3. (Color online) Images of two functionalized cantilever pairs. Streptavidin-coated magnetic beads were exposed to BSA-coated reference arm (top) and B-BSA-coated sensing arm (bottom). (a) System with non-specific binding with more beads on sensing arm than reference arm. (b) System with insignificant nonspecific binding.

other cantilever pair for which the chemistry has worked much more favorably [Fig. 3(b)].

It has been shown previously that for a similar interferometric sensors<sup>14,15</sup> at high frequencies, the resolution was limited by the thermomechanical noise of the cantilever

$$d_{\text{rms}} = \sqrt{\frac{4K_B T \Delta f_{\text{meas}}}{QK\omega_n}}, \quad (1)$$

where  $\omega_n=2\pi f_n$  is the natural frequency,  $K_B$  is the Boltzmann constant,  $T$  is temperature during the measurement,  $\Delta f_{\text{meas}}$  is the detection bandwidth,  $Q$  is the quality factor, and  $K$  is the effective stiffness. We analyzed the minimum detectable signal and its dependence on excitation frequency. The interferometer of the cantilevers was biased at the maximum sensitivity point (208 nm from Fig. 2) and an input signal to actuate cantilevers was applied using an electromagnet (Industrial Magnetics Inc., ER1-202). The power spectral density (PSD) of the signals from the cantilever was recorded. Figure 4(a) illustrates the spectrum when an oscillating magnetic force at 1103 Hz is applied to the cantilever.

Figure 4(b) shows a separately measured PSD (with no excitation) of noise and the MDD. Measurements were performed over the 3–1321 Hz range, in order to observe the transition from flicker to thermomechanical noise while avoiding resonance. In Fig. 4(b), the PSDs of theoretical thermomechanical noise and experimentally measured noise

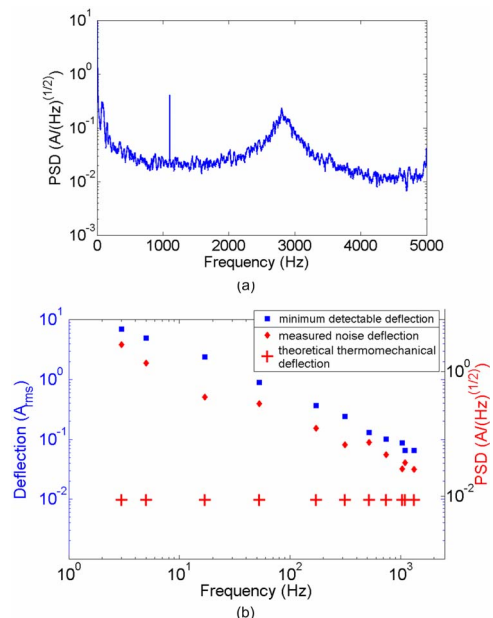


FIG. 4. (Color online) (a) PSD of the output signal when input signal is a sinusoid at 1103 Hz and (b) noise PSD and MDD in the measurement.

are compared (represented by the right-hand ordinate) and the MDD in  $\text{\AA}_{\text{rms}}$  is shown on the left-hand ordinate for a 1 Hz detection bandwidth. The MDD was experimentally determined by continuously reducing the intensity of the magnetic field (until the output signal was small but not less than two to three times the noise). As expected, the MDD decreases with frequency until the flicker noise is no longer significant. We were able to observe  $0.065 \text{\AA}_{\text{rms}}$  of minimum relative displacement between the two cantilevers at 1103 Hz.

As frequency increases the MDD approaches the thermomechanical noise limit. One reason for the difference between calculated thermomechanical noise [Eq. (1)] and the measured noise at high frequencies [plus signs and diamonds in Fig. 4(b)] may be attributed to the assumed material properties of the cantilever. Another possible reason is that the calculation for thermomechanical noise is performed for bare cantilevers whereas the measured noise is for a cantilever with magnetic beads. Further, the interferometer's biasing point may experience small drifts, affecting the calibration for deflection values.

In the presence of a magnetic field, dipole moments induced in magnetic particles result in an applied force. Using the approach of Fisher *et al.*<sup>17</sup> the force applied on a bead under the influence of a magnetic field is expressed by

$$\vec{F} = \frac{\pi d_{\text{bead}}^3}{2\mu_0} \left( \frac{\mu_r - 1}{\mu_r + 2} \right) \vec{B} \frac{d\vec{B}}{dz}, \quad (2)$$

where  $d_{\text{bead}}$  is the diameter of the magnetic bead,  $\mu_0$  is the permeability of free space,  $\mu_r$  is the relative permeability of the magnetic bead,  $B$  is the magnetic field, and  $z$  is the distance between the magnetic bead and electromagnet. Equating the deflection due to magnetic force applied on  $n$  beads ( $d_{\text{rms}} = nF/K$ ) to that resulting from the thermomechanical noise [Eq. (1)] and solving for  $n$  yields

$$n_{\text{min}} = \frac{1.97\mu_0 t}{\pi d_{\text{bead}}^3} \left| \vec{B} \frac{d\vec{B}}{dz} \right| (E\rho)^{1/4} \left( \frac{wK_B T \Delta f_m}{QL} \right)^{1/2} \left( \frac{\mu_r + 2}{\mu_r - 1} \right). \quad (3)$$

Equation (3) represents the theoretical minimum detectable number of beads as a function of the geometric and material properties of the beads and the cantilever as well as the magnetic field properties.

To estimate the numerical value of  $n_{\text{min}}$  for the current case, we used Eq. (3) along with the cantilever properties provided above. The magnetic field of the electromagnet was measured with a gauss meter at various distances from the magnet and its gradient was calculated offline. The resulting product of the magnetic field and gradient was estimated as  $B \times |dB/dz| = 0.511 \times 10^{-3} \text{ T T/m}$  and the force applied to a magnetic bead was calculated as  $2.88 \times 10^{-16} \text{ N}$ . Using the streptavidin-coated superparamagnetic beads from Bangs Labs [ $d_{\text{bead}} = 0.83 \text{ }\mu\text{m}$ , relative permeability  $\mu_r \approx 12.3$  (Ref. 18)], as few as 100 magnetic beads located at the tip of the cantilever can potentially be detected according to Eq. (3).

Considering material properties alone, it is clear that a cantilever with small Young's modulus would result in a more sensitive sensor. Lower material densities would also improve sensitivity. Accordingly, silicon-rich nitride, the material of the cantilevers used in this study is an appropriate choice.

Equation (3) indicates that among the three dimensions of a rectangular cantilever, beam thickness has the strongest effect on sensitivity. Magnetic bead diameter also has a significant impact on sensitivity; fewer beads are required for detection if the bead diameter is increased.

The magnetic field used to actuate the system also has a significant impact on the minimum detectable bead number through both its strength and gradient. From a practical point of view, varying the magnetic field may provide greater flexibility than changing the material and geometric properties of the cantilever provided that the magnet being used is capable of generating such fields.

We demonstrated an analysis of noise and detection limits in immunomagnetic nanomechanical sensors and showed subangstrom level deflection resolution. Our current efforts are directed towards enhancing the detection sensitivity by both designing new, thinner cantilevers and employing new electromagnets with increased magnetic fields. Magnetic beads are promising tools for separation of biomolecules from biological samples<sup>19</sup> and are already widely used. We expect that their combination with cantilevers can enable a system that is highly sensitive and compatible with complex biological mixtures. Our future goal is to use this method to detect low concentrations of biomolecules such as cancer markers and cells from samples such as urine and serum.

This research was funded by the NSF Award No. 0725189. We thank Professor George Chiu in Purdue Mechanical Engineering for access to inkjet dispensing system and Koray Icoz for cantilever drawings.

<sup>1</sup>Y. Arntz, J. D. Seelig, H. P. Lang, J. Zhang, P. Hunziker, J. P. Ramseyer, E. Meyer, M. Hegner, and C. Gerber, *Nanotechnology* **14**, 86 (2003).

<sup>2</sup>J. H. Pei, F. Tian, and T. Thundat, *Anal. Chem.* **76**, 292 (2004).

<sup>3</sup>B. Ilic, D. Czaplewski, H. G. Craighead, P. Neuzil, C. Campagnolo, and C. Batt, *Appl. Phys. Lett.* **77**, 450 (2000).

<sup>4</sup>A. Gupta, D. Akin, and R. Bashir, *J. Vac. Sci. Technol. B* **22**, 2785 (2004).

<sup>5</sup>B. Dhayal, W. A. Henne, D. D. Doornweerd, R. G. Reifengerger, and P. S. Low, *J. Am. Chem. Soc.* **128**, 3716 (2006).

<sup>6</sup>L. Johnson, A. T. K. Gupta, A. Ghafoor, D. Akin, and R. Bashir, *Sens. Actuators B* **115**, 189 (2006).

<sup>7</sup>J. Fritz, M. K. Baller, H. P. Lang, H. Rothuizen, P. Vettiger, E. Meyer, H. J. Guntherodt, C. Gerber, and J. K. Gimzewski, *Science* **288**, 316 (2000).

<sup>8</sup>H. Sone, A. Ikeuchi, T. Izumi, H. Okano, and S. Hosaka, *Jpn. J. Appl. Phys., Part 1* **45**, 2301 (2006).

<sup>9</sup>S. Q. Li, L. Orona, Z. M. Li, and Z. Y. Cheng, *Appl. Phys. Lett.* **88**, 073507 (2006).

<sup>10</sup>A. Gupta, D. Akin, and R. Bashir, *Appl. Phys. Lett.* **84**, 1976 (2004).

<sup>11</sup>S. M. Lindsay, Y. L. Lyubchenko, N. J. Tao, Y. Q. Li, P. I. Oden, J. A. Derose, and J. Pan, *J. Vac. Sci. Technol. A* **11**, 808 (1993).

<sup>12</sup>D. R. Baselt, G. U. Lee, K. M. Hansen, L. A. Chrisey, and R. J. Colton, *Proc. IEEE* **85**, 672 (1997).

<sup>13</sup>Y. Weizmann, F. Patolsky, O. Lioubashevski, and I. Willner, *J. Am. Chem. Soc.* **126**, 1073 (2004).

<sup>14</sup>C. A. Savran, A. W. Sparks, J. Sihler, J. Li, W. C. Wu, D. E. Berlin, T. P. Burg, J. Fritz, M. A. Schmidt, and S. R. Manalis, *J. Microelectromech. Syst.* **11**, 703 (2002).

<sup>15</sup>C. A. Savran, T. P. Burg, J. Fritz, and S. R. Manalis, *Appl. Phys. Lett.* **83**, 1659 (2003).

<sup>16</sup>G. G. Yaralioglu, A. Atalar, S. R. Manalis, and C. F. Quate, *J. Appl. Phys.* **83**, 7405 (1998).

<sup>17</sup>J. K. Fisher, J. R. Cummings, K. V. Desai, L. Vicci, B. Wilde, K. Keller, C. Weigle, G. Bishop, R. M. Taylor, C. W. Davis, R. C. Boucher, E. Timothy O'Brien, and R. Superfine, *Rev. Sci. Instrum.* **76**, 053711 (2005).

<sup>18</sup>S. S. Shevkoplyas, A. C. Siegel, R. M. Westervelt, M. G. Prentiss, and G. M. Whitesides, *Lab Chip* **7**, 1294 (2007).

<sup>19</sup>O. Olsvik, T. Popovic, E. Skjerve, K. S. Cudjoe, E. Hornes, J. Ugelstad, and M. Uhlen, *Clin. Microbiol. Rev.* **7**, 43 (1994).